Unravelling the Open-Shell Character of Peripentacene on Au(111)

Ana Sánchez-Grande, José I. Urgel*, Libor Veis, Shayan Edalatmanesh, José Santos, Koen Lauwaet, Pingo Mutombo, José M. Gallego, Jiri Brabec, Pavel Beran, Dana Nachtigallová, Rodolfo Miranda, Nazario Martín*, Pavel Jelínek*, and David Écija*

Unravelling the open-shell character of peripentacene on Au(111)

Ana Sánchez-Grande,[a] José I. Urgel,[a,] Libor Veis,[b] Shayan Edalatmanesh,[c,d] José Santos,[a,e] Koen Lauwaet,[a] Pingo Mutombo,[c] José M. Gallego,[f] Jiří Brabec,[b] Pavel Beran,[b] Dana Nachtigallová,[d,g] Rodolfo Miranda,[a,h] Nazario Martín,[a,e,*] Pavel Jelínek,[c,d*] and David Écija [a,*]*

a. IMDEA Nanoscience, C/ Faraday 9, Campus de Cantoblanco, 28049 Madrid, Spain.

b. J. Heyrovský Institute of Physical Chemistry, Czech Academy of Sciences, v.v.i., Dolejškova 3, 18223 Prague 8, Czech Republic.

c. Institute of Physics of the Czech Academy of Science, CZ-16253 Praha, Czech Republic.

d. Regional Centre of Advanced Technologies and Materials, Palacký University Olomouc, 771 46 Olomouc, Czech Republic

e. Departamento de Química Orgánica, Facultad de Ciencias Químicas, Universidad Complutense de Madrid, 28040 Madrid, Spain.

f. Instituto de Ciencia de Materiales de Madrid, CSIC, Cantoblanco 28049, Madrid, Spain.

g. Institute of Organic Chemistry and Biochemistry of the Czech Academy of Science, 160 00 Praha, Czech Republic.

h. Departamento de Física de la Materia Condensada, Universidad Autónoma de Madrid, 28049 Madrid, Spain.

*E-mails of the authors for correspondence: david.ecija@imdea.org (D.E.); jose-ignacio.urgel@imdea.org (J.I.U.); nazmar@ucm.es (N.M.); jelinekp@fzu.cz (P.J.).

ABSTRACT

Polycyclic aromatic hydrocarbons (PAHs) are a family of organic compounds comprising two or more fused aromatic rings, which feature manifold applications in modern technology. Among these species, those presenting an open-shell magnetic ground state are of particular interest for organic electronic, spintronic, nonlinear optics and energy storage devices. Within PAHs, special attention has been devoted in recent years to the synthesis and study of the acene and fused acene (periacene) families, steered by their decreasing HOMO-LUMO gap with length and predicted open-shell character above some size. However, an experimental fingerprint of such magnetic ground state has remained elusive.

Here, we report on the in-depth electronic characterization of isolated peripentacene molecules on a Au(111) surface. Scanning tunnelling spectroscopy, complemented by computational investigations, reveals an antiferromagnetic singlet ground state, characterized by singlet-triplet inelastic excitations with an experimental effective exchange coupling (J_{eff}) of 40.5 meV. Our results deepen on the fundamental understanding of organic compounds with magnetic ground states, featuring perspectives in carbon-based spintronic devices.

TOC GRAPHICS

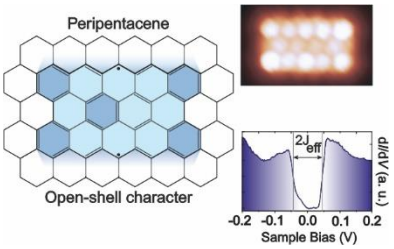

KEYWORDS: surface science, scanning tunneling spectroscopy, periacenes, magnetic exchange-coupling, density functional theory, density matrix renormalization group

Polycyclic aromatic hydrocarbons (PAHs) have been the subject of intensive studies from both experimental and theoretical points of view since the middle of last century.[1] Most of the PAHs reported to date present a stable closed-shell (non-magnetic) electronic configuration in their ground state. However, recent advances in the methods for synthesis and analysis of PAHs have led to the creation of PAHs with an open-shell (antiferromagnetic or ferromagnetic) ground state, conferring them unique electronic, optical and magnetic properties [2–4] While magnetism is generally related to transition metals and lanthanides, the magnetic properties of carbon-based nanostructures have attracted increased attention recently.[5] Their electronic structure has unique dependence on size, geometry and edge-shape with strongly spin-polarized edge states, inherent to the π-electron network, being created at its zigzag edges.[6] Physically, the kinetic energy (hopping), the electrostatic Coulomb and the exchange interaction of valence electrons may lead to closed-shell or open-shell ground states, respectively.

The synthesis of PAHs with open-shell ground states is challenging for organic chemists due to their intrinsic high reactivity which emerges from their unpaired electron spin density. One of the

main driving forces in the formation of such open-shell PAHs is related to the presence of more aromatic sextet rings in their open-shell resonance forms, where the energy needed to break a double bond is compensated by the increased resonance stabilization energy. Importantly, the ground state of periacenes (rectangular graphene fragments formed by fused acenes and comprised of both zigzag and armchair edges, see scheme 1), has been under intensive debate during the last years.[7–13] They can be considered as model compounds to study the size dependent evolution of different physical properties foreseen for graphene nanoribbons, where periacenes larger than peritetracene are predicted to possess an open-shell singlet ground state.[7,14] Up until now, sterically protected peritetracene is the largest member of the periacene family synthetized in solution,[11,12] while only experimental signatures for peripentacene have been suggested by mass spectrometry in the residue after sublimation of pentacene.[15]

Able to side-step reactivity issues, on-surface synthesis has emerged as an appealing playground for the investigation of rationally-designed reactive molecules under ultra-high vacuum (UHV) conditions studied via advanced scanning probe techniques. Recently, the synthesis of several members of the acene,[16–21] indenofluorene,[22,23] anthene[24] and triangulene[25–27] families, together with some zigzag graphene nanoribbons (ZGNRs)[28] has been reported. Nevertheless, successful experimental investigations on periacenes has remained scarce and only recently the synthesis of peritetracene, peripentacene and heteroatom-doped perihexacene on metallic single crystals has been achieved.[13,29,30] Whereas there are theoretical reports on the electronic structure of peripentacene in literature,[7,11] there is a lack of experimental evidence. Here we provide, to the best of our knowledge, the first description via scanning tunnelling spectroscopy of the Coulomb gap of peripentacene on Au(111) under UHV conditions,[29] while revealing its open-shell character and its preservation on a metallic substrate, which is manifested as singlet-triplet

inelastic excitations. Our experimental results are supported by spin-polarized density functional theory (DFT) and *ab initio* density matrix renormalization group (DMRG) calculations, which reveal the antiferromagnetic open-shell singlet ground state of the peripentacene, shedding light on the fundamental understanding of the open-shell ground state of PAHs with prospects in optoelectronic and spintronic devices.

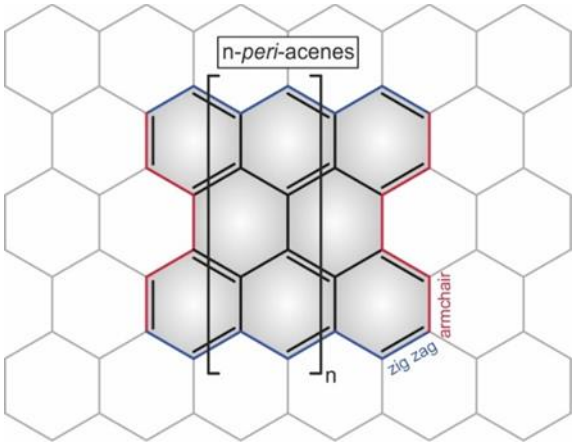

Scheme 1. Chemical structure of periacenes and their structural relationship to graphene.

To study the electronic structure of pristine peripentacene, we sublimed 13,13'-bis(dibromomethylene)-13*H*,13'*H*-6,6'-bipentacenylidene (**1**) onto an atomically clean Au(111) surface held at room temperature and subsequently annealed at 180 °C. Annealing samples at such temperature affords the thermal cyclodehydrogenation of the *peri*-positions of **1** as well as the cleavage of dibromomethylene functional groups, which gives rise to the formation of a minority of peripentacene monomers as a side product coexisting with the formation, via homocoupling, of diradical one-dimensional peripentacene polymers, as recently reported by our group (see Figure 1a for the synthetic route toward the formation of peripentacene polymers and

molecules).[31] Herein, the formation of individual peripentacene molecules after the annealing step is attributed to hydrogen passivation of the radical sites associated with the presence of residual hydrogen gas in the vacuum chamber.[32,33] Figure 1b shows a high-resolution STM image of a rectangle-shaped nanostructure compatible with a peripentacene molecule. To confirm the chemical structure of the molecule observed in Figure 1b, an ultrahigh-resolution STM (UHR-STM) image acquired with a CO-functionalized tip was recorded in the Pauli repulsion regime (Figure 1c).[7,8] Hereby, intramolecular features corresponding to a peripentacene molecular backbone are clearly distinguished.[29] The experimental features of the individual peripentacene molecule observed in Figure 1c are in agreement with the planar conformation of the molecular species given by the DFT-optimized geometry on the Au(111) surface (Figure 1d), which shows an adsorption height of 3.3 Å with respect to the underlying gold surface. Figure 1e shows spin-polarized DFT calculations performed in order to evaluate the electronic ground state of the free-standing molecule. The maximum spin density for the molecule is located at the zigzag edges with the largest amplitude on the central zigzag carbon atoms, in agreement with previous *ab initio* DMGR calculations.[11]

In addition, our calculations reveal an antiferromagnetic open-shell singlet ground state (total spin S = 0), over the ferromagnetic open-shell triplet (see Table S1 and S3). Also the non-magnetic closed-shell states is few eV higher in energy with respect to the open-shell singlet ground state depending on method. At this point a rather simple, but intuitive comment regarding the Clar's sextet rule[36] and the role of the Kekulé and the non-Kekulé structures in the radical character of periacenes is convenient. While the Kekulé structure of peripentacene presents two migrating aromatic sextets, the non-Kekulé diradical resonance structure of peripentacene admits five aromatic sextets by breaking one π-bond, resulting in two unpaired

electrons, which leads to a gain in aromatic stabilization energy. In addition to the interplay between energy penalty for breaking a π-bond and aromatic energy gain, the degeneracies of the non-Kekulé structures of the peripentacene molecule should be taken into account in order to evaluate its radical character, as recently reported by Yeh and Chai[37] (see Figure S1 where a closed-shell Kekulé and an open-shell non-Kekulé diradical structures of peripentacene are shown).

Next, the electronic structure of peripentacene is probed on Au(111) via STS (Figure 1f,g). Voltage-dependent differential conductance spectra (dI/dV vs. V) acquired with a CO-functionalized tip on a peripentacene molecule show resonances in the local density of states (LDOS) at −1000 mV, −470 mV, 700 mV and 960 mV (highlighted with grey dashed lines in Figure 1f). Experimental constant-current dI/dV maps acquired at the respective energies evidence an excellent agreement with the simulated dI/dV maps of the HOMO−1, SOMO, SUMO, and LUMO+1 molecular orbitals (MO) with a CO-tip[38] for a free-standing peripentacene molecule (Figure 1h). Therefore, we found an experimental Coulomb gap of 1170 meV deduced from the energy separation between single occupied MOs, *i.e.* SOMO and SUMO (see Figure S2 for the calculated energy diagram of the peripentacene). Interestingly, having a closer look to the energy region near the Fermi level (Figure 1g) we observed an abrupt stepwise change in conductance, which is symmetric around the Fermi energy at ±40.5 meV, indicative of an inelastic excitation[39] (see Figure 1i for the short range dI/dV maps and Figure S6b for the threshold extracted from the d^2I/dV^2 spectrum derived from Figure 1g). Such an inelastic excitation, together with the presence of single occupied MOs, evidences the magnetic ground state of the molecule and, as we will discuss in the following, is assigned to a singlet-triplet magnetic excitation due to the tunnelling electrons. The differences in the zig-zag region

between the SOMO/SUMO and spin excitation d*I*/d*V* maps are assigned to selection rules for the tunneling current between the electronic states of peripentacene molecule and CO-tip, as well as to distinct tip-height setpoints for acquiring the d*I*/d*V* maps under comparison (see Supporting Information for full discussion). Only recently, inelastic excitations have been observed for other graphene-like nanostructures designed and adsorbed on surfaces,[40–43] though this is, to the best of our knowledge, the first visualization of such excitations for a member of the periacene family investigated on a surface.

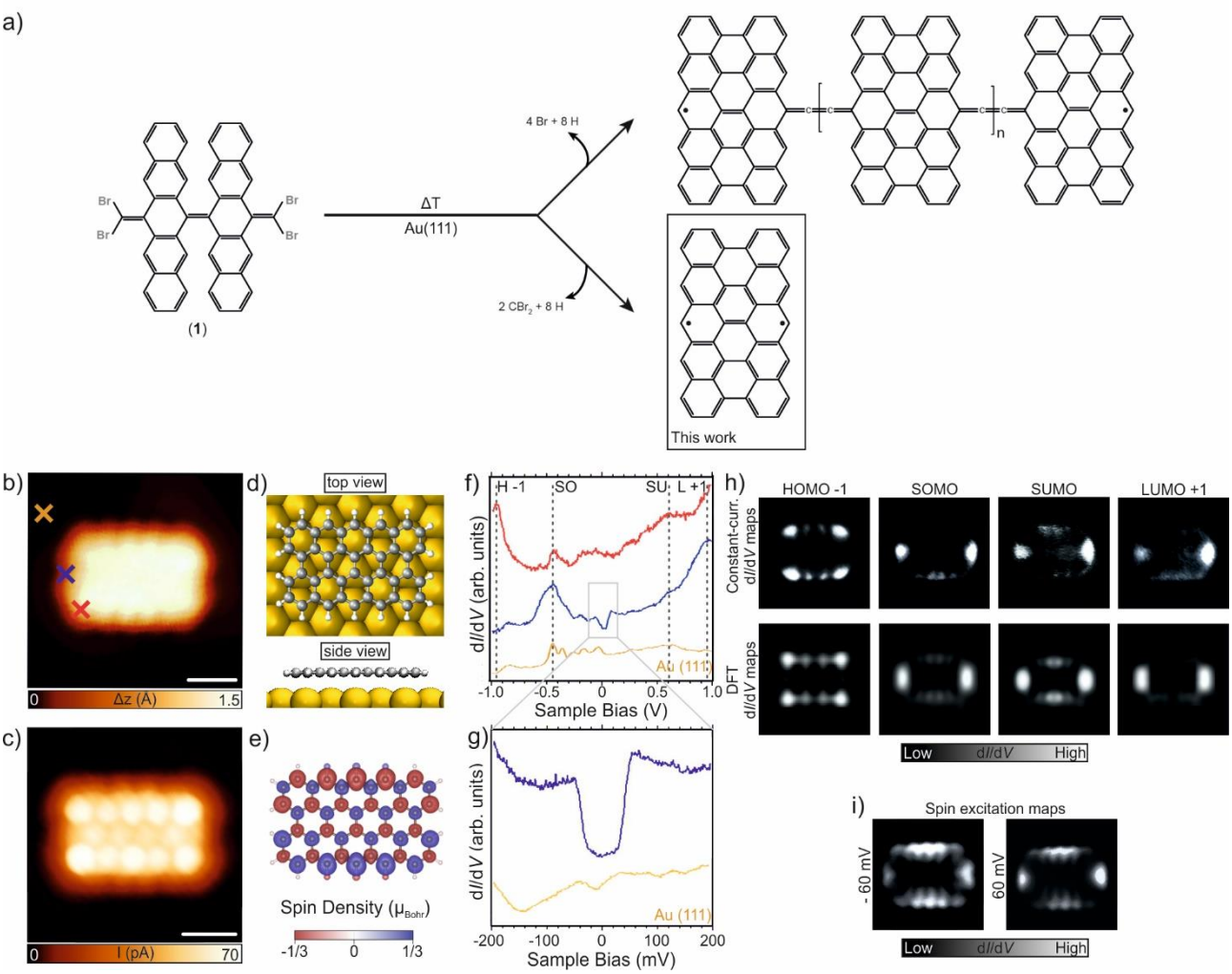

Figure 1. On-surface synthesis and electronic characterization of peripentacene on Au(111). a) Synthesis scheme of diradical peripentacene polymers and peripentacene monomers on Au(111). b) High-resolution STM topography image of a peripentacene molecule after annealing precursor (**1**) at 180°C. V_b = -60 mV, I_t = 150 pA, scale bar = 1 nm. c) Constant-height ultrahigh-resolution STM image acquired with a CO-functionalized tip showing intramolecular features attributed to peripentacene molecule. Open- feedback parameters 3 mV, 5 pA. Scale bars: 1 nm. d) Top (upper panel) and side (lower panel) views of the DFT equilibrium geometry of the peripentacene on Au(111). e) Calculated spin density distribution of a free standing peripentacene using DFT-B3LYP. Spin polarizations of opposite signs appear at the zig zag edges. f) Differential conductance spectra on selected positions of the peripentacene molecule; the red and blue curves were acquired at the corner and apex positions of the molecule, as indicated in the constant-current STM images in (b). The orange curve corresponds to the reference dI/dV spectrum acquired on Au(111). g) Zoom-in differential conductance spectra taken from (f) where an abrupt stepwise change in conductance around the Fermi energy is observed. See Figure S6a,b for the fittings of the dI/dV shown in (g) and the d^2I/dV^2 spectra respectively. h) Top panel: dI/dV maps acquired at the peaks labelled H −1, SO, SU and L +1 in (f). Bottom panel: corresponding DFT calculated dI/dV maps at the energetic positions corresponding to H −1, SO, SU and L +1. Tunneling parameters for the dI/dV maps: H −1 (V_b = -1.0 V, I_t = 150 pA); SO (V_b = -0.47 V, I_t = 150 pA); SU (V_b = 0.65 V, I_t = 150 pA) and L+1 (V_b = 0.90 V, I_t = 150 pA). i) dI/dV maps acquired at $V_b = \pm 60$ mV, I_t = 150 pA revealing the physical location of the inelastic spin excitations of the molecule. Open feedback parameters for dI/dV spectra: (f) V_b = -1.0 V, I_t = 150 pA, V_{rms} = 16 mV; (g) V_b = 0.2 V, I_t = 250 pA, V_{rms} = 8 mV. Every experimental image was acquired at 4.3 K.

Unrestricted DFT[44] calculations reveal a singlet (S=0) open-shell ground state for a free-standing peripentacene, whereas the triplet (S=1) state is higher in energy in the range of 20-100 meV depending on the employed DFT functional (see Table 1 in SI). We have also performed DFT-PBE simulations of the peripentacene molecule on the Au(111) surface to estimate the effect of the metallic surface on its diradical character. The calculation reveals that the peripentacene molecule conserves the open-shell singlet state as the ground state. However, the difference between the singlet and triplet energies reduces by ≈30% with respect to the gas-phase calculation with the same exchange-correlation functional to 15 meV. This indicates that the additional screening driven by the proximity of the metal surface reduces the singlet-triplet excitation energy.

Additionally, we have explored the nature of the molecular ground state using high-level wave-function-based electronic structure theory, *i.e.* DMRG calculations, employing the full π active space comprising 44 p_z carbon orbitals. Herein, our calculations for free-standing peripentacene molecule corroborate an open-shell singlet ground state, with a computed singlet-triplet gap of 130 meV, which is much larger than the experimental value. This discrepancy can be caused by two effects: i) the presence of the metallic substrate substantially reduces the molecular gap[45] and ii) an absence of correlations effects in DMRG calculations including excitations outside the π active space.

To address the influence of the proximity of the metal surface on the singlet-triplet gap of the peripentacene we have scaled its HOMO-LUMO gap with scissors operator.[46,47] A reduction of the HOMO-LUMO gap by ≈15% is manifested itself in the reduced DMRG singlet-triplet gap of 101 meV (Table 2 in SI). In order to estimate the effect of the dynamical correlation missing in

the DMRG calculations (excitations outside the π active space), we have performed supplementary multireference coupled cluster calculations with single and double excitations (see Supporting Information) in the π active space and in the full orbital space, and used the difference between the two singlet-triplet gaps as a dynamical correlation correction (52 meV, Table 3 in SI). The final estimate of the singlet-triplet gap based on the DMRG results with the scaled HOMO-LUMO gap and corrected by the effect of dynamical correlation corresponds to 49 meV, in an excellent agreement with the experimental value. This analysis shows that the exchange coupling scales proportionally with the molecular gap and the dynamical correlations beyond the π active space play important role.

Notably, the DMRG occupation numbers of natural orbitals reveal the diradical open-shell nature of peripentacene (see Supporting Information, Figure S9), in agreement with previous calculations.[11] Thus, our experimental and theoretical findings reveal that peripentacene species on Au(111) present a singlet open-shell ground state, with an experimental singlet-triplet excitation energy (exchange coupling) of J_{eff} = 40.5 meV, significantly larger than the J_{eff} found in other nanographenes formed on Au(111).[40]

It is noteworthy mentioning that several peripentacene molecules present a different aspect, especially noticeable in UHR-STM images. Such species are usually located at the elbows of the herringbone ridges of the Au(111) surface. Figure 2a shows a UHR-STM image recorded at low bias sample where six brighter lobes at one of the zigzag edges of the molecule reveals an enhancement of the local density of states (LDOS); while the opposite zigzag edge presents a considerable loss of resolution, tentatively attributed to the bonding of the carbon at the apical position of the central benzene ring of the molecule to the elbow region of the herringbone ridges of the Au(111) surface (see chemical structure proposed in Figure 2b). Additionally, differential

conductance dI/dV spectra recorded at low bias voltages (Figure 2c) at the high LDOS locations (zigzag edge of the molecule which is not bounded to the gold surface) show prominent zero-bias peaks, attributed to a Kondo resonance (S = ½).[35,40] The rather strong interaction of molecules presenting a large open-shell character with the underlying surface has been recently reported for other graphene-like nanostructures,[17,22,40] where the registry of the molecules with the surface plays an important role for their electronic and magnetic properties. We also detect a minority of species on the surface where the central carbon atoms at both edges are saturated, i.e. extra-hydrogenated, by two hydrogen atoms. We have investigated the possibility of generating the peripentacene molecule from the extra-hydrogenated species via STM single atom manipulation. We have located the CO-functionalized tip at one of the central carbon atoms at one edge and turn off the feedback loop (setpoint conditions: V_b = 200 mV and I_t = 50 pA). Subsequently, the tunneling voltage V_b is increased to ≈ 2.0 V for a few seconds, and an abrupt change in the tunneling current is detected, which is attributed to the manipulation event (see Figure S7).[13,17]

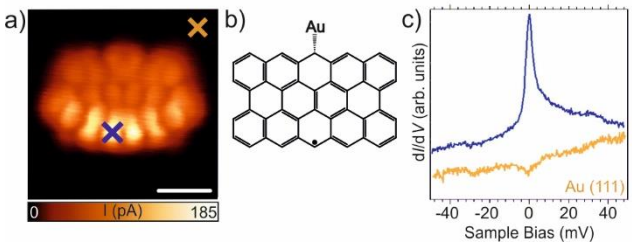

Figure 2. Au-peripentacene on Au(111). a) Constant-height ultrahigh-resolution STM image acquired with a CO-functionalized tip at 4.3 K showing intramolecular features attributed to peripentacene molecule bounded to gold at one of the zig zag edges. Open- feedback parameters 3 mV, 5 pA. Scale bars: 0.5 nm. b) Chemical sketch of the Au-peripentacene system shown in (a). c) dI/dV spectra showing the Kondo resonance at the unbound end of the molecule (blue line). Reference spectrum is taken on the bare Au(111) surface (orange line). Open feedback

parameters: V_b = 0.05 V, I_t = 150 pA, V_{rms} = 0.8 mV. See Figure S6c for the fitting of the Kondo resonance shown in (c).

In conclusion, we have performed an in-depth characterization of the electronic structure of the peripentacene molecule on Au(111) via STS, complemented with DFT and DMRG calculations. Annealing precursor (**1**) at 180°C induces the cyclodehydrogenation and cleavage of dibromomethylene moieties, giving rise to the on-surface formation of peripentacene coexisting with diradical one-dimensional polymers. The peripentacene molecule presents an experimental electronic gap of 1170 meV. DFT and multiconfigurational DMRG calculations reveal its antiferromagnetic singlet open-shell ground state, which is experimentally manifested as a singlet-triplet inelastic excitation, featuring a relatively strong exchange-coupling of 40.5 meV. Notably, several peripentacene molecules show a different aspect noticeable in UHR-STM images. Some of them present prominent zero-bias peaks attributed to a Kondo resonance (S = ½), while a minority of species appear passivated by two hydrogen atoms at the central carbon atom of both edges. Our work reveals the open-shell antiferromagnetic ground state of the largest member of the periacene family synthetized to date. We expect that our findings are of general relevance for the study of open-shell PAHs with perspectives in optoelectronic and spintronic devices.

ASSOCIATED CONTENT

Supporting Information. Experimental methods. Synthesis scheme of diradical peripentacene polymers and peripentacene monomers on Au(111). Chemical sketch of Kekulé and non-Kekulé resonance forms of the peripentacene molecule. Schematic unrestricted spin diagram and

corresponding frontier orbitals of a dimer plotted for the spin-up and spin-down configurations. On-surface generation of peripentacene via STM atom manipulation of extra-hydrogenated species on Au(111). Details of DFT calculations on peripentacene monomer. Details of DMRG and MR CCSD calculations on peripentacene monomer.

Notes

The authors declare no competing financial interest.

ACKNOWLEDGMENT

This project has received funding from the European Research Council (ERC) under the European Union's Horizon 2020 research and innovation programme (grant agreement No 766555). We acknowledge Comunidad de Madrid [projects QUIMTRONIC-CM (Y2018/NMT-4783), MAD2D and NanoMagCost], and Ministerio de Ciencia, Innovación y Universidades (projects SpOrQuMat, CTQ2017-83531-R and CTQ2016-81911-REDT). IMDEA Nanociencia thanks support from the "Severo Ochoa" Programme for Centers of Excellence in R&D (MINECO, Grant SEV-2016-0686). We acknowledge support from Praemium Academie of the Academy of Science of the Czech Republic, GACR 18-09914S and and CzechNanoLab Research Infrastructure supported by MEYS CR (LM2018110). J.I.U thanks the JCB Atracción de Talento program from Comunidad de Madrid (contract no. IND-12535). L.V. acknowledges support from the Czech Science Foundation (18-18940Y) and Center for Scalable and Predictive methods for Excitation and Correlated phenomena (SPEC), which was funded by the U.S. Department of Energy (DOE), Office of Science, Office of Basic Energy Sciences, the Division of Chemical Sciences, Geosciences, and Biosciences. This work was also supported by The

Czech Ministry of Education, Youth and Sports from the Large Infrastructures for Research, Experimental Development and Innovations project „e-Infrastructure CZ – LM2018140“.

REFERENCES

(1) Clar, E.; Schoental, R. *Polycyclic Hydrocarbons*; Springer, 1964; Vol. 2.
(2) Sun, Z.; Zeng, Z.; Wu, J. Zethrenes, Extended p-Quinodimethanes, and Periacenes with a Singlet Biradical Ground State. *Acc. Chem. Res.* **2014**, *47* (8), 2582–2591.
(3) Sun, Z.; Wu, J. Closed-Shell and Open-Shell 2D Nanographenes. In *Polyarenes I*; Siegel, J. S., Wu, Y.-T., Eds.; Topics in Current Chemistry; Springer Berlin Heidelberg, 2012; pp 197–248.
(4) Das, S.; Wu, J. Polycyclic Hydrocarbons with an Open-Shell Ground State. *Physical Sciences Reviews* **2017**, *2* (5).
(5) Narita, A.; Wang, X.-Y.; Feng, X.; Müllen, K. New Advances in Nanographene Chemistry. *Chem. Soc. Rev.* **2015**, *44* (18), 6616–6643. https://doi.org/10.1039/C5CS00183H.
(6) Enoki, T.; Kobayashi, Y.; Fukui, K.-I. Electronic Structures of Graphene Edges and Nanographene. *International Reviews in Physical Chemistry* **2007**, *26* (4), 609–645.
(7) Mizukami, W.; Kurashige, Y.; Yanai, T. More π Electrons Make a Difference: Emergence of Many Radicals on Graphene Nanoribbons Studied by *Ab Initio* DMRG Theory. *J. Chem. Theory Comput.* **2013**, *9* (1), 401–407.
(8) Horn, S.; Plasser, F.; Müller, T.; Libisch, F.; Burgdörfer, J.; Lischka, H. A Comparison of Singlet and Triplet States for One- and Two-Dimensional Graphene Nanoribbons Using Multireference Theory. *Theor Chem Acc* **2014**, *133* (8), 1511.
(9) Moscardó, F.; San-Fabián, E. On the Existence of a Spin-Polarized State in the n-Periacene Molecules. *Chemical Physics Letters* **2009**, *480* (1–3), 26–30.
(10) Horn, S.; Lischka, H. A Comparison of Neutral and Charged Species of One- and Two-Dimensional Models of Graphene Nanoribbons Using Multireference Theory. *The Journal of Chemical Physics* **2015**, *142* (5), 054302.
(11) Ni, Y.; Gopalakrishna, T. Y.; Phan, H.; Herng, T. S.; Wu, S.; Han, Y.; Ding, J.; Wu, J. A Peri-Tetracene Diradicaloid: Synthesis and Properties. *Angewandte Chemie International Edition* **2018**, *57* (31), 9697–9701.
(12) Ajayakumar, M. R.; Fu, Y.; Ma, J.; Hennersdorf, F.; Komber, H.; Weigand, J. J.; Alfonsov, A.; Popov, A. A.; Berger, R.; Liu, J.; Müllen, K.; Feng, X. Toward Full Zigzag-Edged Nanographenes: Peri-Tetracene and Its Corresponding Circumanthracene. *J. Am. Chem. Soc.* **2018**, *140* (20), 6240–6244.
(13) Mishra, S.; Lohr, T. G.; Pignedoli, C. A.; Liu, J.; Berger, R.; Urgel, J. I.; Müllen, K.; Feng, X.; Ruffieux, P.; Fasel, R. Tailoring Bond Topologies in Open-Shell Graphene Nanostructures. *ACS Nano* **2018**, *12* (12), 11917–11927.
(14) Jiang, D.; Sumpter, B. G.; Dai, S. First Principles Study of Magnetism in Nanographenes. *The Journal of Chemical Physics* **2007**, *127* (12), 124703.
(15) Roberson, L. B.; Kowalik, J.; Tolbert, L. M.; Kloc, C.; Zeis, R.; Chi, X.; Fleming, R.; Wilkins, C. Pentacene Disproportionation during Sublimation for Field-Effect Transistors. *J. Am. Chem. Soc.* **2005**, *127* (9), 3069–3075.

(16) Urgel, J. I.; Hayashi, H.; Di Giovannantonio, M.; Pignedoli, C. A.; Mishra, S.; Deniz, O.; Yamashita, M.; Dienel, T.; Ruffieux, P.; Yamada, H.; Fasel, R. On-Surface Synthesis of Heptacene Organometallic Complexes. *J. Am. Chem. Soc.* **2017**, *139* (34), 11658–11661.
(17) Urgel, J. I.; Mishra, S.; Hayashi, H.; Wilhelm, J.; Pignedoli, C. A.; Giovannantonio, M. D.; Widmer, R.; Yamashita, M.; Hieda, N.; Ruffieux, P.; Yamada, H.; Fasel, R. On-Surface Light-Induced Generation of Higher Acenes and Elucidation of Their Open-Shell Character. *Nat Commun* **2019**, *10* (1), 1–9.
(18) Zuzak, R.; Dorel, R.; Krawiec, M.; Such, B.; Kolmer, M.; Szymonski, M.; Echavarren, A. M.; Godlewski, S. Nonacene Generated by On-Surface Dehydrogenation. *ACS Nano* **2017**, *11* (9), 9321–9329.
(19) Zuzak, R.; Dorel, R.; Kolmer, M.; Szymonski, M.; Godlewski, S.; Echavarren, A. M. Higher Acenes by On-Surface Dehydrogenation: From Heptacene to Undecacene. *Angewandte Chemie International Edition* **2018**, *57* (33), 10500–10505.
(20) Eisenhut, F.; Kühne, T.; García, F.; Fernández, S.; Guitián, E.; Pérez, D.; Trinquier, G.; Cuniberti, G.; Joachim, C.; Peña, D.; Moresco, F. Dodecacene Generated on Surface: Reopening of the Energy Gap. *ACS Nano* **2020**, *14* (1), 1011–1017.
(21) Krüger, J.; García, F.; Eisenhut, F.; Skidin, D.; Alonso, J. M.; Guitián, E.; Pérez, D.; Cuniberti, G.; Moresco, F.; Peña, D. Decacene: On-Surface Generation. *Angew. Chem.* **2017**, *129* (39), 12107–12110.
(22) Di Giovannantonio, M.; Eimre, K.; Yakutovich, A. V.; Chen, Q.; Mishra, S.; Urgel, J. I.; Pignedoli, C. A.; Ruffieux, P.; Müllen, K.; Narita, A.; Fasel, R. On-Surface Synthesis of Antiaromatic and Open-Shell Indeno[2,1-b]Fluorene Polymers and Their Lateral Fusion into Porous Ribbons. *J. Am. Chem. Soc.* **2019**, *141* (31), 12346–12354.
(23) Di Giovannantonio, M.; Urgel, J. I.; Beser, U.; Yakutovich, A. V.; Wilhelm, J.; Pignedoli, C. A.; Ruffieux, P.; Narita, A.; Müllen, K.; Fasel, R. On-Surface Synthesis of Indenofluorene Polymers by Oxidative Five-Membered Ring Formation. *J. Am. Chem. Soc.* **2018**, *140* (10), 3532–3536.
(24) Konishi, A.; Hirao, Y.; Matsumoto, K.; Kurata, H.; Kishi, R.; Shigeta, Y.; Nakano, M.; Tokunaga, K.; Kamada, K.; Kubo, T. Synthesis and Characterization of Quarteranthene: Elucidating the Characteristics of the Edge State of Graphene Nanoribbons at the Molecular Level. *J. Am. Chem. Soc.* **2013**, *135* (4), 1430–1437. https://doi.org/10.1021/ja309599m.
(25) Pavliček, N.; Mistry, A.; Majzik, Z.; Moll, N.; Meyer, G.; Fox, D. J.; Gross, L. Synthesis and Characterization of Triangulene. *Nature Nanotech* **2017**, *12* (4), 308–311.
(26) Mishra, S.; Beyer, D.; Eimre, K.; Liu, J.; Berger, R.; Gröning, O.; Pignedoli, C. A.; Müllen, K.; Fasel, R.; Feng, X.; Ruffieux, P. Synthesis and Characterization of π-Extended Triangulene. *J. Am. Chem. Soc.* **2019**.
(27) Su, J.; Telychko, M.; Hu, P.; Macam, G.; Mutombo, P.; Zhang, H.; Bao, Y.; Cheng, F.; Huang, Z.-Q.; Qiu, Z.; Tan, S. J. R.; Lin, H.; Jelínek, P.; Chuang, F.-C.; Wu, J.; Lu, J. Atomically Precise Bottom-up Synthesis of π-Extended [5]Triangulene. *Science Advances* **2019**, *5* (7), eaav7717.
(28) Ruffieux, P.; Wang, S.; Yang, B.; Sánchez-Sánchez, C.; Liu, J.; Dienel, T.; Talirz, L.; Shinde, P.; Pignedoli, C. A.; Passerone, D.; Dumslaff, T.; Feng, X.; Müllen, K.; Fasel, R. On-Surface Synthesis of Graphene Nanoribbons with Zigzag Edge Topology. *Nature* **2016**, *531* (7595), 489–492.
(29) Rogers, C.; Chen, C.; Pedramrazi, Z.; Omrani, A. A.; Tsai, H.-Z.; Jung, H. S.; Lin, S.; Crommie, M. F.; Fischer, F. R. Closing the Nanographene Gap: Surface-Assisted Synthesis

of Peripentacene from 6,6′-Bipentacene Precursors. *Angewandte Chemie International Edition* **2015**, *54* (50), 15143–15146.
(30) Wang, X.-Y.; Dienel, T.; Di Giovannantonio, M.; Barin, G. B.; Kharche, N.; Deniz, O.; Urgel, J. I.; Widmer, R.; Stolz, S.; De Lima, L. H.; Muntwiler, M.; Tommasini, M.; Meunier, V.; Ruffieux, P.; Feng, X.; Fasel, R.; Müllen, K.; Narita, A. Heteroatom-Doped Perihexacene from a Double Helicene Precursor: On-Surface Synthesis and Properties. *J. Am. Chem. Soc.* **2017**, *139* (13), 4671–4674.
(31) Sánchez-Grande, A.; Urgel, J. I.; Cahlík, A.; Santos, J.; Edalatmanesh, S.; Rodríguez-Sánchez, E.; Lauwaet, K.; Mutombo, P.; Nachtigallová, D.; Nieman, R.; Lischka, H.; de la Torre, B.; Miranda, R.; Gröning, O.; Martín, N.; Jelínek, P.; Écija, D. Diradical Organic One-dimensional Polymers Synthesized on a Metallic Surface. *Angew. Chem. Int. Ed.* **2020**, anie.202006276.
(32) Urgel, J. I.; Di Giovannantonio, M.; Gandus, G.; Chen, Q.; Liu, X.; Hayashi, H.; Ruffieux, P.; Decurtins, S.; Narita, A.; Passerone, D.; Yamada, H.; Liu, S.; Müllen, K.; Pignedoli, C. A.; Fasel, R. Overcoming Steric Hindrance in Aryl-Aryl Homocoupling via On-Surface Copolymerization. *ChemPhysChem* **2019**, *20* (18), 2360–2366.
(33) Eisenhut, F.; Lehmann, T.; Viertel, A.; Skidin, D.; Krüger, J.; Nikipar, S.; Ryndyk, D. A.; Joachim, C.; Hecht, S.; Moresco, F.; Cuniberti, G. On-Surface Annulation Reaction Cascade for the Selective Synthesis of Diindenopyrene. *ACS Nano* **2017**, *11* (12), 12419–12425.
(34) Weiss, C.; Wagner, C.; Kleimann, C.; Rohlfing, M.; Tautz, F. S.; Temirov, R. Imaging Pauli Repulsion in Scanning Tunneling Microscopy. *Phys. Rev. Lett.* **2010**, *105* (8), 086103.
(35) Kichin, G.; Weiss, C.; Wagner, C.; Tautz, F. S.; Temirov, R. Single Molecule and Single Atom Sensors for Atomic Resolution Imaging of Chemically Complex Surfaces. *Journal of the American Chemical Society* **2011**, *133* (42), 16847–16851.
(36) Clar, E. *The Aromatic Sextet. 1972*; John Wiley & Sons: New York, NY.
(37) Yeh, C.-N.; Chai, J.-D. Role of Kekulé and Non-Kekulé Structures in the Radical Character of Alternant Polycyclic Aromatic Hydrocarbons: A TAO-DFT Study. *Scientific Reports* **2016**, *6*, srep30562.
(38) Krejčí, O.; Hapala, P.; Ondráček, M.; Jelínek, P. Principles and Simulations of High-Resolution STM Imaging with a Flexible Tip Apex. *Phys. Rev. B* **2017**, *95* (4), 045407.
(39) Hirjibehedin, C. F.; Lutz, C. P.; Heinrich, A. J. Spin Coupling in Engineered Atomic Structures. *Science* **2006**, *312* (5776), 1021.
(40) Mishra, S.; Beyer, D.; Eimre, K.; Kezilebieke, S.; Berger, R.; Gröning, O.; Pignedoli, C. A.; Müllen, K.; Liljeroth, P.; Ruffieux, P.; Feng, X.; Fasel, R. Topological Frustration Induces Unconventional Magnetism in a Nanographene. *Nat. Nanotechnol.* **2020**, *15* (1), 22–28.
(41) Mishra, S.; Beyer, D.; Berger, R.; Liu, J.; Gröning, O.; Urgel, J. I.; Müllen, K.; Ruffieux, P.; Feng, X.; Fasel, R. Topological Defect-Induced Magnetism in a Nanographene. *J. Am. Chem. Soc.* **2020**, *142* (3), 1147–1152.
(42) Li, J.; Sanz, S.; Corso, M.; Choi, D. J.; Peña, D.; Frederiksen, T.; Pascual, J. I. Single Spin Localization and Manipulation in Graphene Open-Shell Nanostructures. *Nat Commun* **2019**, *10* (1), 1–7.
(43) Mishra, S.; Yao, X.; Chen, Q.; Eimre, K.; Groening, O.; Ortiz, R.; Di Giovannantonio, M.; Sancho-Garcia, J. C.; Fernandez-Rossier, J.; Pignedoli, C. A.; Muellen, K.; Ruffieux, P.; Narita, A.; Fasel, R. Giant Magnetic Exchange Coupling in Rhombus-Shaped Nanographenes with Zigzag Periphery. *arXiv:2003.03577 [cond-mat]* **2020**.

(44) Blum, V.; Gehrke, R.; Hanke, F.; Havu, P.; Havu, V.; Ren, X.; Reuter, K.; Scheffler, M. Ab Initio Molecular Simulations with Numeric Atom-Centered Orbitals. *Computer Physics Communications* **2009**, *180* (11), 2175–2196.
(45) Neaton, J. B.; Hybertsen, M. S.; Louie, S. G. Renormalization of Molecular Electronic Levels at Metal-Molecule Interfaces. *Phys. Rev. Lett.* **2006**, *97* (21), 216405..
(46) Abad, E.; Dappe, Y. J.; Martínez, J. I.; Flores, F.; Ortega, J. C $_6$ H $_6$ /Au(111): Interface Dipoles, Band Alignment, Charging Energy, and van Der Waals Interaction. *The Journal of Chemical Physics* **2011**, *134* (4), 044701.
(47) Abad, E.; Ortega, J.; Dappe, Y. J.; Flores, F. Dipoles and Band Alignment for Benzene/Au(111) and C60/Au(111) Interfaces. *Appl. Phys. A* **2009**, *95* (1), 119–124.
(48) Ternes, M.; Heinrich, A. J.; Schneider, W.-D. Spectroscopic Manifestations of the Kondo Effect on Single Adatoms. *J. Phys.: Condens. Matter* **2008**, *21* (5), 053001.